

Multiple Bad Data Identification Considering Measurement Dependencies

Eduardo Caro, *Student Member, IEEE*, Antonio J. Conejo, *Fellow, IEEE*, Roberto Mínguez, Marija Zima, *Member, IEEE*, and Göran Andersson, *Fellow, IEEE*

Abstract—This paper analyzes the multiple bad data originated by a gross error in any voltage or current transformer of the measurement equipment. Considering the statistical correlations among measurements, an identification algorithm based on the largest normalized residual test is specifically designed to deal with multiple bad data. Two case studies are analyzed and conclusions duly drawn.

Index Terms—Dependent measurements, multiple bad data identification, power system state estimation.

I. INTRODUCTION

A. Motivation and Aim

IN any electric energy system, the control center regularly performs a state estimation to compute the most likely state of the network, fundamentally based on the measurement set transferred from each substation. One of the most relevant features of any estimation algorithm is to detect and to identify the presence of bad data.

Although measurements are routinely considered independent, some studies indicate that this hypothesis is inaccurate, since the signals from the voltage/current transformers are processed and combined to obtain the power flow and voltage measurements that the state estimator employs. From this point of view, if an error occurs in a voltage or current transformer, more than one “processed measurement” is generally corrupted, leading a measurement set populated with multiple bad data.

To the best of our knowledge, no bad data detection and identification algorithm has been specifically designed to consider dependencies among measurements. However, if statistical correlations are properly considered in the identification procedure,

a more reliable and robust bad data identification can be achieved. To develop such procedure is the aim of the work reported in this paper.

B. Contributions

The contribution of this paper is threefold: first, to study the influence over the measurement set of a gross error affecting any current or voltage transformer; second, to check the performance of the traditional detection and identification algorithms in the presence of multiple bad data; and third, to propose a modification of the well-known identification method based on the largest normalized residual (LNR) test in order to improve its robustness if multiple bad data are present.

C. Literature Review

Within the framework of power system state estimation, methods and solution algorithms are well documented. The pioneering work is due to Schweppe *et al.* [1]–[3] and others [4]–[6].

The capability of bad data detection and identification is a key element of any estimator. Some studies focus on parameter error identification [7], [8], topology error identification [9]–[12] and, mainly, measurement error identification.

The elimination of bad data in the measurement set can be addressed by the use of robust estimators: least absolute value [13], least median of squares [14], etc. Concerning the widely-used weighted least of squares (WLS) estimator, two methods are available [6]: the LNR test and the hypothesis testing identification.

References [15] and [16] describe and analyze an advanced SCADA system. Reference [17] analyzes the measurement dependencies due to measurement transformer influence and proposes a technique to compute the measurement correlation coefficients based on the point estimate method. Finally, [18] proposes an estimation algorithm that considers these dependencies.

D. Paper Organization

The rest of this paper is organized as follows: Section II analyzes the measurement system and provides expressions to compute the relative error of processed measurements. Section III discusses the drawbacks of traditional methods and Section IV proposes a identification algorithm capable of identifying multiple bad data. Section V analyzes two insightful case studies and, finally, Section VI provides some relevant conclusions.

II. MEASUREMENT SYSTEM: DESCRIPTION AND MODEL

In any electric power system, the control center regularly performs a state estimation of the network state using the consid-

Manuscript received February 22, 2010; revised September 20, 2010 and March 15, 2011; accepted May 15, 2011. Date of publication June 09, 2011; date of current version October 21, 2011. The work of E. Caro, A. J. Conejo, and R. Mínguez was supported in part by Junta de Comunidades de Castilla—La Mancha (JCCM) through project POH11-0102-0275 and by the Ministry of Education and Science of Spain through CICYT Project DPI2009-09573. Additionally, the work of E. Caro was supported in part by the Education and Science Council of JCCM; and the work of R. Mínguez was supported in part by the Spanish Ministry of Science and Innovation (MCI) through the Ramon y Cajal program. Paper no. TPWRS-00137-2010.

E. Caro and A. J. Conejo are with the Universidad de Castilla-La Mancha, Ciudad Real, Spain (e-mail: Eduardo.Caro@uclm.es; Antonio.Conejo@uclm.es).

R. Mínguez is with the Environmental Hydraulics Institute IH Cantabria, Universidad de Cantabria, Cantabria, Spain (e-mail: Roberto.Minguez@unican.es).

M. Zima and G. Andersson are with ETH Zürich, Zürich, Switzerland (e-mail: bockarjova@eeh.ee.ethz.ch; andersson@eeh.ee.ethz.ch).

Color versions of one or more of the figures in this paper are available online at <http://ieeexplore.ieee.org>.

Digital Object Identifier 10.1109/TPWRS.2011.2157366

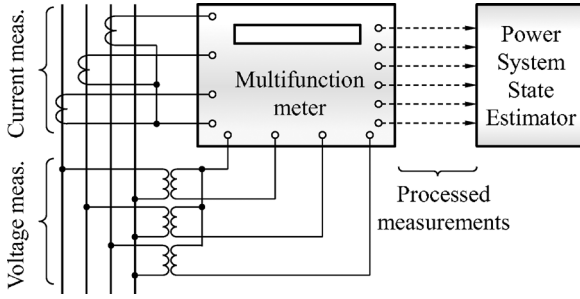


Fig. 1. Voltage and current signal connections in a three-phase measuring configuration.

ered system model and its parameters, and the measurement data collected from all the substations located throughout the network.

A. Measurement Infrastructure

Each substation transmits to the control center, using an electronic equipment called remote terminal unit (RTU), a measurement set usually formed by bus voltages and active/reactive line power flows. This information is generally obtained from a multifunction meter, which collects the analogic signals from a set of current/voltage transformers, processes them digitally, and generates the measurement data that the estimator uses. Thus, from the viewpoint of the multifunction meter, measurements can be classified into two groups:

- *input measurements*, which are those measurements directly captured from the actual physical system;
- *processed measurements*, which are the data digitally generated by the multifunction meter, transmitted to the control center, and used by the state estimator.

There are some different connection configurations for the measurement equipment [17]. Fig. 1 provides a scheme of the widely-used three-phase configuration, in which the multifunction meter is connected to three voltage/current transformers.

For the sake of simplicity and without loss of generality, a three-phase configuration is considered throughout the study reported in this paper.

B. Signal Processing

The internal software routines implemented in the multifunction meter [19] allow computing the output data under the presence of nonfundamental harmonics. Assuming a sinusoidal system state, those equations can be simplified as

$$V_i = F_{V_i}(\cdot) = \frac{V_i^A + V_i^B + V_i^C}{3} \quad (1)$$

$$P_{ij} = F_{P_{ij}}(\cdot) = \sum_{f=\{A,B,C\}} V_i^f I_{ij}^f \cos(\psi_{ij}^f) \quad (2)$$

$$Q_{ij} = F_{Q_{ij}}(\cdot) = \sum_{f=\{A,B,C\}} V_i^f I_{ij}^f \sin(\psi_{ij}^f) \quad (3)$$

where V_i^f is the voltage signal for phase f and bus i , and I_{ij}^f and ψ_{ij}^f are the current and voltage-current angle signals for phase f and line ij at terminal i .

From (1)–(3), note that some input signals are required in several equations simultaneously. Therefore, if one of this shared

input data is corrupted by a gross error, several processed measurements are inaccurately computed. In other words, a single gross error in a voltage/current transformer spreads over several processed measurements, provoking multiple interacting bad data.

Equations (1)–(3) can consider unbalanced and/or asymmetric states. For the sake of clarity, hereinafter balanced symmetric working conditions are assumed.

C. Measurement Error Model

Reference [18] analyzes the measurement dependency and proposes a method to compute the correlation coefficient between measurements. This technique is used in this paper. Notwithstanding the nonlinearities of (1)–(3), it has been numerically verified that the assumption of linear-dependency between measurements is sufficiently accurate [18].

The measurement vector z that the estimator uses (i.e., the vector of processed measurements) can be expressed as

$$z = z^{\text{true}} + e \quad (4)$$

where z^{true} is the true measurement vector and e is the measurement error vector. Vector e can be statistically characterized as a Gaussian-distributed linearly-dependent variable vector. Therefore, vector e can be expressed as

$$e = L_z v \quad (5)$$

where v is a vector of standard independent Gaussian random variables, and L_z is the lower-triangular Cholesky factor of the measurement variance-covariance matrix C_z , i.e., $C_z = L_z L_z^T$. For more information, see [18, Appendix].

From (4) and (5), it readily follows

$$\begin{bmatrix} z_1 \\ \vdots \\ z_i \\ \vdots \\ z_m \end{bmatrix} = \begin{bmatrix} z_1^{\text{true}} \\ \vdots \\ z_i^{\text{true}} \\ \vdots \\ z_m^{\text{true}} \end{bmatrix} + \begin{bmatrix} l_{11} & & & & \\ \vdots & \ddots & & & \mathbf{0} \\ l_{i1} & \dots & l_{ii} & & \\ \vdots & \vdots & \vdots & \ddots & \\ l_{m1} & \dots & l_{mi} & \dots & l_{mm} \end{bmatrix} \begin{bmatrix} v_1 \\ \vdots \\ v_i \\ \vdots \\ v_m \end{bmatrix} \quad (6)$$

where l_{ij} is the ij component of matrix L_z . In a real-world system, the majority of l_{ij} coefficients are equal to zero, because measurement dependency can only be found between measurements within each substation.

Providing a normalized Gaussian random vector v , (6) can be used to generate measurement sets involving a realistic dependency, consistent with the routines implemented in the multifunction meter. Note that a gross error in component v_i spreads over measurement z_j if l_{ji} is different from zero.

D. Relative Error Computation

From (1)–(3), note that there are three types of input data variables: voltage magnitude, current magnitude, and voltage-current phase angle (V_i^f , I_{ij}^f , and ψ_{ij}^f , respectively). Depending on which type of input measurement is corrupted by a gross error, the processed measurements are affected in one way or another. For example, if an error occurs in a current (or phase angle) input measurement, some of the active/reactive power flow measurements are affected, whereas the voltage processed measurement

TABLE I
RELATIVE ERRORS OF PROCESSED MEASUREMENTS

	$\varepsilon_r(V_i)$	$\varepsilon_r(P_{ij})$	$\varepsilon_r(Q_{ij})$
$V_i^{f,\text{bad}}$	$100 \frac{M\sigma_V}{3 V_i^{f,\text{true}} }$	$100 \frac{M\sigma_V}{3 V_i^{f,\text{true}} }$	$100 \frac{M\sigma_V}{3 V_i^{f,\text{true}} }$
$I_{ij}^{f,\text{bad}}$	0	$100 \frac{M\sigma_I}{3 I_{ij}^{f,\text{true}} }$	$100 \frac{M\sigma_I}{3 I_{ij}^{f,\text{true}} }$
$\psi_{ij}^{f,\text{bad}}$	0	$100 \frac{ \cos(\psi_{ij}^{f,\text{true}} + M\sigma_\psi) - \cos(\psi_{ij}^{f,\text{true}}) }{3 \cos(\psi_{ij}^{f,\text{true}})}$	$100 \frac{ \sin(\psi_{ij}^{f,\text{true}} + M\sigma_\psi) - \sin(\psi_{ij}^{f,\text{true}}) }{3 \sin(\psi_{ij}^{f,\text{true}})}$

is not. Note that just one bad input measurement can affect more than one processed measurement and, thus, it can produce a measurement set populated with multiple bad data.

The relative error of a z_i processed measurement caused by a bad p_j input measurement is computed as follows:

$$\varepsilon_{p_j}(z_i) = 100 \left| \frac{F_{z_i}(\mathbf{p}^{\text{true}}) - F_{z_i}(\mathbf{p}^{\text{bad}})}{F_{z_i}(\mathbf{p}^{\text{true}})} \right| \quad (7)$$

where

$$\mathbf{p}^{\text{bad}} = [p_1^{\text{true}}, \dots, p_j^{\text{true}} + M\sigma_j, \dots, p_n^{\text{true}}]^T \quad (8)$$

and the functional vector $F_{z_i}(\cdot)$ represents the equation implemented in the multifunction meter software to compute the processed measurement z_i (1)–(3), and M is the number of the standard deviations of the input measurement gross error magnitude.

Assuming a balanced sinusoidal system operation, Table I provides the expressions to compute the relative error of the V_i , P_{ij} , and Q_{ij} processed measurements (columns) if a bad measurement occurs in V_i^f , I_{ij}^f , ψ_{ij}^f input measurements (rows), respectively.

Considering that the standard deviations of input measurements are known parameters, the relative errors in Table I can be plotted using tridimensional graphs. (Standard deviations used are: $\sigma_V = \sigma_I = \sigma_\psi = 0.01$ pu.)

Fig. 2 provides the graphical characterization of those relative errors. Each tridimensional plot provides the relative error in processed measurements (V_i , P_{ij} , and Q_{ij}) if an M -magnitude gross error is added to each type of input data: V_i^f , I_{ij}^f , and ψ_{ij}^f .

The following observations are in order:

- 1) Fig. 2(a) provides the relative error of processed measurements in case of a gross error affecting any input measurement V_i^f . Note that the three types of processed measurements behave identically.
- 2) Fig. 2(b) provides the relative error of processed measurements in case of a gross error affecting any input measurement I_{ij}^f . Note that processed measurements P_{ij} and Q_{ij} are distorted similarly, whereas the measurement V_i is not influenced.
- 3) Fig. 2(c) provides the relative error of processed measurements in case of a gross error affecting any input measurement ψ_{ij}^f . For the sake of clarity, the surface $\varepsilon_{\psi_{ij}^f}(V_i)$ is not plotted, since its value is always zero. Note that processed measurements P_{ij} and Q_{ij} are distorted similarly, while measurement V_i is not influenced.

From Fig. 2, it can be concluded that the magnitudes of the relative errors in processed measurements are not very high

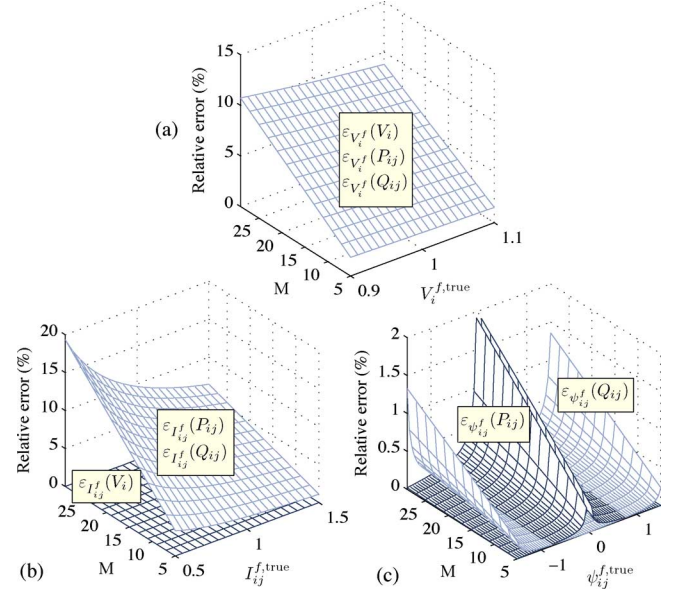


Fig. 2. Relative errors in processed measurements.

(due to the fact that processed measurements are computed using error-free parameters but the one under study). However, those relative errors are large enough to deteriorate the estimation accuracy and, consequently, the detection/identification algorithms can fail in the presence of those multiple bad measurements.

III. STATE ESTIMATION AND BAD DATA IDENTIFICATION

Most state estimators in practical use are based on a mathematical optimization problem which minimizes an objective function J , which usually can be expressed as a function of vector $\mathbf{y} = \mathbf{z} - \mathbf{h}(\mathbf{x})$, where \mathbf{x} is the state vector and $\mathbf{h}(\cdot)$ is a nonlinear functional vector, such that $\mathbf{h}(\mathbf{x}^{\text{true}}) = \mathbf{z}^{\text{true}}$.

For example, the WLS approach can be expressed as

$$\underset{\mathbf{x}}{\text{minimize}} \quad J = [\mathbf{z} - \mathbf{h}(\mathbf{x})]^T \mathbf{W} [\mathbf{z} - \mathbf{h}(\mathbf{x})] \quad (9)$$

$$= \mathbf{y}^T \mathbf{W} \mathbf{y} \quad (10)$$

subject to

$$\mathbf{c}(\mathbf{x}) = \mathbf{0}, \mathbf{g}(\mathbf{x}) \leq \mathbf{0} \quad (11)$$

where \mathbf{W} is the weighting matrix, $\mathbf{c}(\mathbf{x})$ are the equality constraints representing perfectly accurate measurements (zero-injection buses), and $\mathbf{g}(\mathbf{x})$ are inequality constraints used to represent physical operating limits. The estimated state, computed

as the solution of problem (9)–(11), is denoted as \mathbf{x}^* , and it is assumed to be close enough to the true state.

Matrix \mathbf{W} is computed as the inverse of the measurement variance-covariance matrix considered (\mathbf{C}_{est}), i.e.,

$$\mathbf{W} = [\mathbf{C}_{\text{est}}]^{-1}. \quad (12)$$

Note that the traditional WLS estimator considers the measurement variance matrix as diagonal (\mathbf{C}_{WLS}), whereas the dependent weighted least squares (DWLS) approach reported in [18] considers additionally the nondiagonal terms (\mathbf{C}_{DWLS}). Hereinafter, it is considered that $\mathbf{C}_{\text{DWLS}} = \mathbf{C}_z$, and $\mathbf{C}_{\text{WLS}} = \text{diag}(\mathbf{C}_z)$.

It can be shown (see [18]) that the computation of matrix \mathbf{C}_z is robust and its coefficients do not vary significantly in case of either multiple bad measurements or Gaussian noise with large standard deviation. However, if matrix \mathbf{C}_z is wrongly estimated, the performance of the proposed approach can be significantly deteriorated, as shown in Section V-A3.

The objective function J can be expressed as

$$\begin{aligned} J &= \mathbf{y}^T [\mathbf{C}_{\text{est}}]^{-1} \mathbf{y} = \mathbf{y}^T [\mathbf{L}_{\text{est}} \mathbf{L}_{\text{est}}^T]^{-1} \mathbf{y} \\ &= (\mathbf{L}_{\text{est}}^{-1} \mathbf{y})^T (\mathbf{L}_{\text{est}}^{-1} \mathbf{y}) = \mathbf{u}^T \mathbf{u} \end{aligned} \quad (13)$$

where \mathbf{L}_{est} is the lower-triangular Cholesky factor of matrix \mathbf{C}_{est} and vector \mathbf{u} is computed as $\mathbf{u} = \mathbf{L}_{\text{est}}^{-1} \mathbf{y}$. Function J follows a Chi-square distribution [4].

A. Bad Data Detection

The Chi-square test for bad data detection can be applied in a simple manner. At the true state \mathbf{x}^{true}

$$\begin{aligned} \mathbf{u} &= \mathbf{L}_{\text{est}}^{-1} \mathbf{y} = \mathbf{L}_{\text{est}}^{-1} [\mathbf{z} - \mathbf{h}(\mathbf{x}^{\text{true}})] \\ &= \mathbf{L}_{\text{est}}^{-1} \mathbf{e} = \mathbf{L}_{\text{est}}^{-1} \mathbf{L}_z \mathbf{v}. \end{aligned} \quad (14)$$

If the DWLS estimator is used, note that $\mathbf{u} = \mathbf{v}$ and the objective function J follows a χ^2 distribution with $m + p - n$ degrees of freedom, where n is the number of state variables and p is the number of equality constraints and active inequality constraints. Bad data detection is a hypothesis testing problem: the null hypothesis \mathcal{H}_0 corresponds to the case in which no bad data are present; and the alternative hypothesis \mathcal{H}_1 corresponds to \mathcal{H}_0 not being true. If J^* is the sum of squared residuals at the estimated state, then

$$J^* \begin{cases} \leq \chi_{m+p-n, \alpha}^2 & \text{accept } \mathcal{H}_0 \\ > \chi_{m+p-n, \alpha}^2 & \text{reject } \mathcal{H}_0 \end{cases} \quad (15)$$

where $\chi_{m+p-n, \alpha}^2$ is the Chi-square distribution function corresponding to a detection confidence level with probability α .

If the WLS estimator is employed, the nondiagonal elements of the variance-covariance matrix are disregarded. In this case, the objective function J still follows a Chi-square distribution but the degrees of freedom change because the dependencies between measurements are eliminated [20].

Both detection and identification traditional algorithms are well documented in the technical literature, e.g., in [4] and [6].

B. Bad Data Identification

If bad data are detected, bad measurements are identified applying the traditional largest normalized residual (LNR) test. The LNR test can be viewed as a hypothesis testing problem, as detailed in [4]. This procedure is composed of the following steps:

- 1) Solve the estimation problem (9)–(11), and compute the normalized residual vector \mathbf{r}^N .
- 2) If the largest normalized residual is larger than the chosen identification threshold (e.g., 3.0), the corresponding measurement is suspected as bad data: go to step 3). Else, the procedure concludes.
- 3) Eliminate the suspected measurement from the measurement set and go to step 1).

The normalized residual r_i^N can be computed as [21]

$$r_i^N = |z_i - h_i(\mathbf{x}^*)| / \sqrt{\Omega_{ii}} \quad (16)$$

where

$$\Omega = \mathbf{C}_z - \mathbf{H}(\mathbf{H}^T \mathbf{W} \mathbf{H})^{-1} \mathbf{H}^T \quad (17)$$

and \mathbf{H} is the Jacobian of function $\mathbf{h}(\mathbf{x})$ evaluated at the optimal estimate, i.e.,

$$\mathbf{H} = \left. \frac{\partial \mathbf{h}(\mathbf{x})}{\partial \mathbf{x}} \right|_{\mathbf{x}=\mathbf{x}^*}. \quad (18)$$

Note that the detection and identification processes can be performed simultaneously bypassing the Chi-square test and computing directly the normalized residuals. However, the calculation of the normalized residuals is computationally expensive and this cost may justify the use of the Chi-square test for preliminary bad measurement detection.

C. Discussion

From the previous subsection, note that if a bad measurement is identified in step 2), it is directly removed from the measurement set in step 3) and the estimation problem (9)–(11) is solved again neglecting this bad measurement.

Section II-D above shows that a gross error affecting any input measurement spreads over one or more processed measurements, following a particular pattern defined by the measurement variance-covariance matrix. Therefore, if a measurement is suspected to be corrupted by a gross error, other correlated measurements are likely to be affected.

The traditional approach removes the suspected bad measurement and its corresponding column/row from the matrix \mathbf{W} , which results in the loss of the correlation information between the removed measurement and other same-substation measurements. As an alternative to this, the proposed method makes use of the correlation coefficients to remove from the correlated measurements the dispersed multiple gross error.

IV. PROPOSED BAD DATA IDENTIFICATION

The aim of the proposed technique is to identify correctly the bad measurements by removing the effect of dispersed multiple bad data.

The proposed identification algorithm is based on the traditional one (see Section III-B), but the state estimation in step 1) is modified to eliminate the multiple bad data which corrupt correct measurements. This modification involves the following considerations:

- 1) Suspected bad data are not removed from the measurement set.
- 2) Problem (9)–(11) is modified in such a way that the suspected bad data do not “weight” in the objective function J , and the error affecting correlated measurements is removed.

The above can be achieved by an adjustment of the weighting matrix \mathbf{W} , rendering matrix \mathbf{W}^* that is computed as

$$\mathbf{W}^* = [\mathbf{I}^* \mathbf{L}_{\text{DWLS}}^{-1}]^T [\mathbf{I}^* \mathbf{L}_{\text{DWLS}}^{-1}] \quad (19)$$

where \mathbf{I}^* is formed as the $m \times m$ identity matrix whose rows corresponding to suspected bad measurements are removed. Thus, vector \mathbf{u} is computed as $\mathbf{u} = \mathbf{I}^* \mathbf{L}_{\text{est}}^{-1} \mathbf{y}$.

Using this weighting matrix, the elements of vector \mathbf{u} are normalized independent Gaussian-distributed variables without the influence of the suspected gross input measurement error.

A. Proposed Algorithm

The proposed algorithm is composed of the following steps:

- 1) An empty set for suspected bad data Ω_{BD} is defined, and the weighting matrix is computed as $\mathbf{W}^* = \mathbf{C}_{\text{DWLS}}^{-1}$.
- 2) Solve the estimation problem (9)–(11) using the weighting matrix \mathbf{W}^* , and compute the normalized residual vector \mathbf{r}^{N} .
- 3) Find the k th measurement with the largest normalized residual r_k^{N} as in (16).
- 4) If r_k^{N} is larger than the chosen identification threshold (e.g., 3.0), the k th measurement is suspected as bad data: go to step 5). Else, the procedure concludes.
- 5) The k th measurement is added to set Ω_{BD} , and matrix \mathbf{W}^* is recomputed using (19). Go to step 2).

To compute the normalized residuals in step 2), matrix \mathbf{W} is employed, since matrix \mathbf{W}^* is not invertible. It has been numerically proved that this approximation does not deteriorate the method performance.

The proposed approach is mathematically consistent regardless of the number of bad data corrupting the input measurement set. Specifically, the technique is also consistent in case of multiple bad data populating same-substation measurements.

B. Illustrative Analytical Example

In this section, an example is provided to show the derivations and algorithms in Section IV-A.

Three measurements, modeled as linearly-dependent Gaussian-distributed variables, are obtained in a substation: voltage (z_{V_1}) and active/reactive power injections (z_{P_1} and z_{Q_1} , respectively). Assume that the corresponding measurement covariance matrix \mathbf{C}_z and its Cholesky factor are

$$\mathbf{C}_z = \begin{bmatrix} 16 & 4 & 4 \\ 4 & 5 & 3 \\ 4 & 3 & 6 \end{bmatrix} \cdot 10^{-4}, \mathbf{L}_z = \begin{bmatrix} 4 & 0 & 0 \\ 1 & 2 & 0 \\ 1 & 1 & 2 \end{bmatrix} \cdot 10^{-2}.$$

Then, the measurement covariance matrices considered by the WLS and DWLS procedures are

$$\mathbf{C}_{\text{WLS}} = \begin{bmatrix} 16 & 0 & 0 \\ 0 & 5 & 0 \\ 0 & 0 & 6 \end{bmatrix} \cdot 10^{-4}$$

$$\mathbf{C}_{\text{DWLS}} = \begin{bmatrix} 16 & 4 & 4 \\ 4 & 5 & 3 \\ 4 & 3 & 6 \end{bmatrix} \cdot 10^{-4}.$$

The measurement vector \mathbf{z} is computed as

$$\mathbf{z} = \mathbf{h}(\mathbf{x}^{\text{true}}) + \mathbf{e} = \mathbf{h}(\mathbf{x}^{\text{true}}) + \mathbf{L}_z \mathbf{v}$$

$$\begin{bmatrix} z_{V_1} \\ z_{P_1} \\ z_{Q_1} \end{bmatrix} = \begin{bmatrix} h_{V_1}(\mathbf{x}^{\text{true}}) \\ h_{P_1}(\mathbf{x}^{\text{true}}) \\ h_{Q_1}(\mathbf{x}^{\text{true}}) \end{bmatrix} + \begin{bmatrix} 4 & 0 & 0 \\ 1 & 2 & 0 \\ 1 & 1 & 2 \end{bmatrix} \begin{bmatrix} v_1 \\ v_2 \\ v_3 \end{bmatrix} \cdot 10^{-2}$$

$$= \begin{bmatrix} h_{V_1}(\mathbf{x}^{\text{true}}) \\ h_{P_1}(\mathbf{x}^{\text{true}}) \\ h_{Q_1}(\mathbf{x}^{\text{true}}) \end{bmatrix} + \begin{bmatrix} 4v_1 \\ 2v_2 + 1v_1 \\ 2v_3 + 1v_2 + 1v_1 \end{bmatrix} \cdot 10^{-2} \quad (20)$$

where the variables v_1 , v_2 , and v_3 follow normalized independent Gaussian distributions.

1) *State Estimation:* Using the DWLS estimator, the following equations hold true at the true state \mathbf{x}^{true} :

$$\mathbf{u} = \mathbf{L}_{\text{DWLS}}^{-1} \mathbf{y} = \mathbf{L}_{\text{DWLS}}^{-1} \mathbf{e}$$

$$= \mathbf{L}_{\text{DWLS}}^{-1} \mathbf{L}_z \mathbf{v} = \mathbf{v} \quad (21)$$

$$\begin{bmatrix} u_1 \\ u_2 \\ u_3 \end{bmatrix} = \begin{bmatrix} 25 & 0 & 0 \\ -12.5 & 50 & 0 \\ -6.25 & -25 & 50 \end{bmatrix} \cdot \begin{bmatrix} 4 & 0 & 0 \\ 1 & 2 & 0 \\ 1 & 1 & 2 \end{bmatrix} \cdot 10^{-2}$$

$$\cdot \begin{bmatrix} v_1 \\ v_2 \\ v_3 \end{bmatrix} = \begin{bmatrix} v_1 \\ v_2 \\ v_3 \end{bmatrix}$$

$$J_{\text{DWLS}} = \mathbf{u}^T \mathbf{u} = v_1^2 + v_2^2 + v_3^2 \quad (22)$$

where \mathbf{L}_{DWLS} is the Cholesky factor of the covariance matrix \mathbf{C}_{DWLS} . Observe that the objective function J_{DWLS} follows a Chi-square distribution with three degrees of freedom ($J_{\text{DWLS}} \sim \chi_3^2$).

On the other hand, using the WLS estimator, at \mathbf{x}^{true}

$$\mathbf{u} = \mathbf{L}_{\text{WLS}}^{-1} \mathbf{y} = \mathbf{L}_{\text{WLS}}^{-1} \mathbf{e} = \mathbf{L}_{\text{WLS}}^{-1} \mathbf{L}_z \mathbf{v} \neq \mathbf{v} \quad (23)$$

$$\begin{bmatrix} u_1 \\ u_2 \\ u_3 \end{bmatrix} = \begin{bmatrix} 25 & 0 & 0 \\ 0 & 44.7 & 0 \\ 0 & 0 & 40.8 \end{bmatrix} \cdot \begin{bmatrix} 4 & 0 & 0 \\ 1 & 2 & 0 \\ 1 & 1 & 2 \end{bmatrix} \cdot 10^{-2} \cdot \begin{bmatrix} v_1 \\ v_2 \\ v_3 \end{bmatrix}$$

$$= \begin{bmatrix} v_1 \\ 0.45v_1 + 0.89v_2 \\ 0.41v_1 + 0.41v_2 + 0.82v_3 \end{bmatrix}$$

$$J_{\text{WLS}} = \mathbf{u}^T \mathbf{u}$$

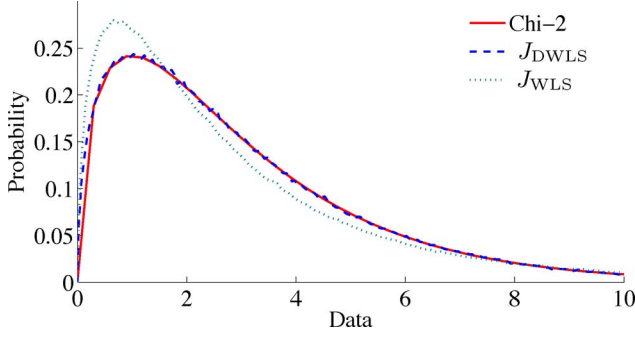


Fig. 3. PDF for the J_{DWLS} and J_{WLS} distributions.

$$= 1.4v_1^2 + 1.1v_1v_2 + 0.67v_1v_3 + 0.97v_2^2 + 0.67v_2v_3 + 0.67v_3^2 \quad (24)$$

where L_{WLS} is the Cholesky factor of matrix C_{WLS} . Observe that the statement $J_{WLS} \sim \chi_3^2$ does not hold true.

From (22) and (24), the statistical characterization of the distributions J_{DWLS} and J_{WLS} can be straightforwardly computed. Fig. 3 depicts the probability density function for J_{DWLS} , J_{WLS} , and χ_3^2 distributions. Observe that the density function of J_{WLS} is significantly different than that corresponding to χ_3^2 .

2) *Gross Error*: Consider that an input measurement is distorted by a gross error whose magnitude is 5 standard deviations. This can be modeled by setting $v_1 = 5$:

$$\begin{bmatrix} z_{V_1} \\ z_{P_1} \\ z_{Q_1} \end{bmatrix} = \begin{bmatrix} h_{V_1}(\mathbf{x}^{\text{true}}) \\ h_{P_1}(\mathbf{x}^{\text{true}}) \\ h_{Q_1}(\mathbf{x}^{\text{true}}) \end{bmatrix} + \begin{bmatrix} 4 \cdot 5 \\ 2v_2 + 5 \\ 2v_3 + 1v_2 + 5 \end{bmatrix} \cdot 10^{-2}.$$

Note that all three measurements are corrupted due to this gross input-measurement error.

Since diagonal terms of matrix L_z are significantly larger than nondiagonal terms, both the traditional and the proposed identification techniques detect z_{V_1} as bad measurement.

Using the traditional identification procedure, measurement z_{V_1} is removed from vector \mathbf{z} , and the resulting vector \mathbf{u} is computed as follows:

$$\begin{bmatrix} u_2 \\ u_3 \end{bmatrix} = L_{WLS}^{-1} \mathbf{e} = L_{WLS}^{-1} L_z \mathbf{v} = \begin{bmatrix} 2.25 + 0.89v_2 \\ 2.05 + 0.41v_2 + 0.82v_3 \end{bmatrix}.$$

Note that the gross error is still affecting vector \mathbf{u} .

On the other hand, using the proposed identification procedure, measurement z_{V_1} is not removed from the measurement set, but it is included on the set of suspected bad data, $\Omega_{BD} = \{z_{V_1}\}$. Matrix I^* is computed as the 3×3 identity matrix whose row corresponding to measurement z_{V_1} is removed. Vector \mathbf{u} is then computed as follows:

$$\mathbf{u} = I^* L_{DWLS}^{-1} \mathbf{e} = I^* L_{DWLS}^{-1} L_z \mathbf{v}, \quad \begin{bmatrix} u_2 \\ u_3 \end{bmatrix} = \begin{bmatrix} 0 & 1 & 0 \\ 0 & 0 & 1 \end{bmatrix} \begin{bmatrix} 25 & 0 & 0 \\ -12.5 & 50 & 0 \\ -6.25 & -25 & 50 \end{bmatrix}$$

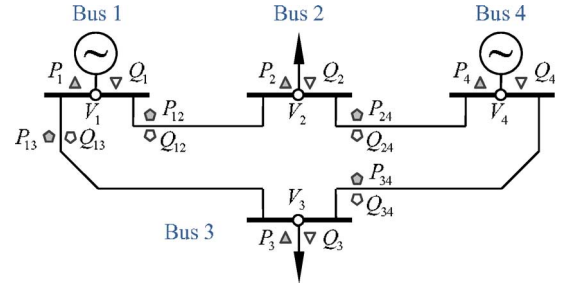


Fig. 4. Four-bus system and measurement configuration.

$$\begin{bmatrix} 4 & 0 & 0 \\ 1 & 2 & 0 \\ 1 & 1 & 2 \end{bmatrix} \cdot 10^{-2} \cdot \begin{bmatrix} v_1 \\ v_2 \\ v_3 \end{bmatrix} \cdot 10^{-2} \cdot \begin{bmatrix} v_1 \\ v_2 \\ v_3 \end{bmatrix} = \begin{bmatrix} v_2 \\ v_3 \end{bmatrix}. \quad (25)$$

Note that the terms of \mathbf{u} follow normalized independent Gaussian distributions. Thus, the gross error does not affect vector \mathbf{u} , i.e., the distortion over same-substation measurements has been removed.

V. CASE STUDY

Two case studies are presented to illustrate the overall performance of the bad data identification method presented in this paper.

A. Four-Bus Case

First case study analyzes in detail a small four-bus system. Fig. 4 depicts the network topology of this system and the measurement configuration considered. In this section, the accuracy of the measurement chain is assumed to be dominantly determined by the measurement transformer, which results in a standard deviation of 0.01 pu.

1) *Introductory Example*: This section illustrates numerically the most relevant aspects of the proposed technique.

Let us assume that a gross error corrupts one of the voltage transformers of substation two, increasing the true voltage value in 20 standard deviations. Consider that 100 measurement scenarios are generated adding zero-mean Gaussian-distributed random errors to the true values computed by a converged power flow solution. In all these scenarios, the same gross error affects the same transformer. The obtained measurement vector is denoted as \mathbf{z} .

For each measurement scenario, vector \mathbf{u} is computed as

$$\mathbf{u} = L_{\text{est}}^{-1} (\mathbf{z} - \mathbf{h}(\mathbf{x}^{\text{true}})) = L_{\text{est}}^{-1} (\mathbf{z} - \mathbf{z}^{\text{true}}) \quad (26)$$

where \mathbf{z}^{true} is the true measurement vector from the power flow solution and L_{est} corresponds either to L_{WLS} or to L_{DWLS} , depending on the estimator employed. Fig. 5 provides the box plot of vector \mathbf{u} for all measurement scenarios, and for both estimators. The range $\pm 3\sigma$ is indicated by dotted lines.

The following observations are in order:

- 1) From the upper plot in Fig. 5 (WLS), note that all components of vector \mathbf{u} corresponding to measurements from

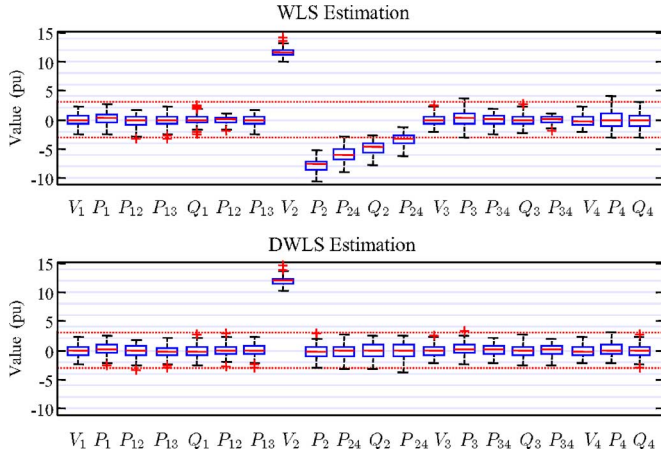

 Fig. 5. Values of \mathbf{u} function using WLS and DWLS estimators.

 TABLE II
 PERFORMANCE OF THE ESTIMATORS

		Iteration:	0	1 st	2 nd	3 rd
WLS	Removed	–	V_2	V_2, P_4	V_2, P_4, Q_4	
	LNR test	V_2	P_4	Q_4	–	
DWLS	Set Ω_{BD}	–	V_2			
	LNR test	V_2	–			

 TABLE III
 TRUE AND ESTIMATED STATE VECTOR

Bus	\mathbf{V}^{true}	$\mathbf{V}^*_{\text{WLS}}$	$\mathbf{V}^*_{\text{DWLS}}$	$\boldsymbol{\theta}^{\text{true}}$	$\boldsymbol{\theta}^*_{\text{WLS}}$	$\boldsymbol{\theta}^*_{\text{DWLS}}$
1	1.0000	0.9988	1.0004	0.0000	0.0000	0.0000
2	0.9824	0.9797	0.9831	-0.0170	-0.0185	-0.0165
3	0.9690	0.9691	0.9699	-0.0327	-0.0316	-0.0324
4	1.0200	1.0219	1.0203	0.0266	0.0299	0.0266

the substation two, are out of the range $[-3\sigma, +3\sigma]$. Thus, the measurements provided by substation two form a set of multiple bad data.

- On the other hand, from the lower plot in Fig. 5 (DWLS), all components of vector \mathbf{u} are located within the aforementioned range, except one measurement: V_2 .

Using the traditional WLS estimator, if V_2 is removed from the measurement set and box plots are plotted again, the components of vector \mathbf{u} have the same value as in Fig. 5 (except for the measurement V_2 that exists no more). Similarly, applying the proposed algorithm to the DWLS estimator, the components of vector \mathbf{u} have the same values as in the lower plot in Fig. 5.

However, if the estimator DWLS is considered and measurement V_2 is directly removed from the measurement set (without the recomputation of matrix \mathbf{W}^*), all the correlation information about the multiple bad data is lost, and the DWLS estimator provides a vector \mathbf{u} which behaves as in the upper plot in Fig. 5.

The traditional and the proposed bad data identification algorithms (detailed in Section III-B and C, respectively) are applied to a randomly-selected measurement scenario. Table II provides the results concerning the iteration number required and the measurements identified as bad data. Table III provides the true voltage magnitudes and angles, and the final estimates for both estimators. Finally, Table IV provides the average relative error

 TABLE IV
 AVERAGE RELATIVE ERRORS (%)

Meas.	WLS	DWLS	Meas.	WLS	DWLS	Meas.	WLS	DWLS
ε_V	0.15	0.06	ε_P	4.73	1.06	ε_{PF}	7.04	1.54
ε_θ	8.13	1.29	ε_Q	5.23	1.27	ε_{QF}	7.51	1.23

for the estimated variables: voltage magnitudes and angles, active/reactive power injections, and active/reactive power flows.

The following observations are in order:

- From Table II, note that the traditional algorithm requires a larger number of iterations. Additionally, several good measurements are removed along with the bad one. The remaining measurements are corrupted by nondetectable conforming multiple bad data.
- From Tables III and IV, note that the quality of the final estimate is significantly better using the DWLS estimator and the proposed identification technique.

For the sake of brevity, results of applying the traditional identification technique to the DWLS estimator are not provided. In this case, results are very similar to the ones provided for the WLS estimator.

2) *Statistical Analysis of the Algorithm Performance:* In order to obtain statistically sound conclusions, the method performance is analyzed using multiple measurement scenarios.

Two types of scenarios are considered:

- A gross error is located in one of the voltage transformers (randomly chosen) of a randomly-selected substation.
- A gross error is randomly located in a voltage or in a current transformer (of a randomly-selected substation).

Note that scenario type b) is more realistic than type a) since, in a real-world system, gross errors affects indistinctively both current and voltage transformers. The magnitude of the gross error considered is 20 standard deviations for both types of scenarios.

Two sets of 100 measurement scenarios are generated and performance results are provided both in Fig. 6 and Table V:

- Fig. 6(a) provides the number of rejected measurements using the traditional and the proposed methodologies (labeled as WLS and DWLS, respectively), for both types of scenarios [labeled as (a) and (b), respectively].
- Fig. 6(b) provides the number of good measurements which have been misidentified, for both methodologies and both cases.
- Table V provides the average relative error computed considering all scenarios.

The following observations are in order:

- From Fig. 6(a), note that the proposed estimator generally requires just one or two iterations, whereas the traditional one needs more.
- From Fig. 6(b), note that the number of misidentifications using the proposed method is insignificant. On the other hand, note that in case of using the traditional one, it is likely than one or more good measurements are removed from the measurement set.
- From Table V, note that the relative errors of the proposed method are notably smaller than those of the traditional one.

3) *Influence of Matrix \mathbf{C}_{DWLS} :* The adequate performance of the proposed method relies on the assumption that matrix \mathbf{C}_{DWLS} has been properly estimated. If the considered covariance matrix does not correspond with the actual measurement-

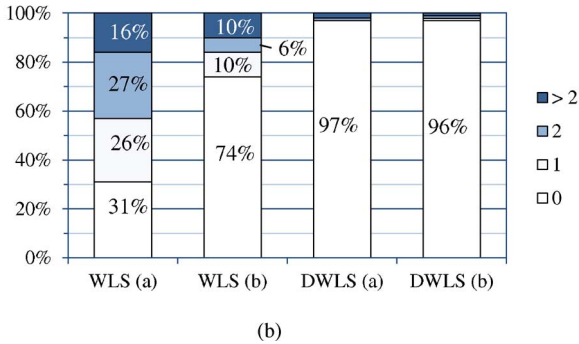
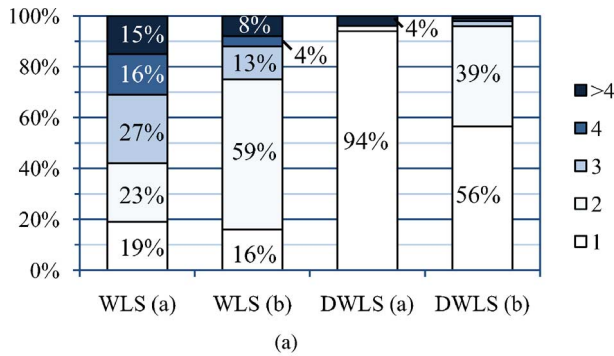


Fig. 6. Identification performance in a four-bus system. (a) Number of suspected/rejected measurements. (b) Number of misidentifications.

TABLE V
AVERAGE RELATIVE ERRORS (%)

Measurement	WLS (a)	WLS (b)	DWLS (a)	DWLS (b)
ϵ_V	0.58	0.48	0.54	0.45
ϵ_θ	9.07	5.28	2.08	2.42
ϵ_P	4.76	2.68	1.07	1.14
ϵ_Q	4.79	2.97	1.22	1.40
ϵ_{PF}	7.02	3.87	1.52	1.76
ϵ_{QF}	7.14	4.18	1.65	1.97

dependency structure, the numerical behavior of the proposed algorithm can be significantly deteriorated.

To illustrate this limitation, a set of 100 measurement scenarios is generated and the proposed estimation and identification DWLS algorithms are applied considering a wrongly-computed measurement covariance matrix C_{DWLS} . In each scenario, the input measurement set of a randomly-chosen substation is corrupted by a gross error of 20 standard deviations. Additionally, the coefficients of the estimated covariance matrix C_{DWLS} corresponding to this substation are intentionally altered with a distortion up to 200%. It is observed that:

- 1) Although the number of iterations does not vary significantly (the variation is smaller than 3%), the average number of misidentifications increases up to seven times.
- 2) Consequently, the average relative error for the estimates increases about ten times.

The previous results highlight the need of using an accurate estimate of the measurement covariance matrix C_{DWLS} .

B. 39-Bus Case

This section analyzes the performance of the proposed procedure applied to a larger case study: a 39-bus system. Two sets of 100 measurement scenarios are generated as in Section V-A2 [cases (a) and (b)], but three gross errors affect three different

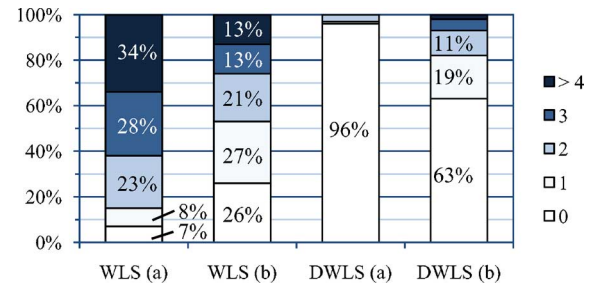


Fig. 7. Number of misidentifications in the 39-bus system.

TABLE VI
AVERAGE RELATIVE ERRORS (%)

Meas.	Scenario (a)			Scenario (b)		
	WLS	WLS*	DWLS	WLS	WLS*	DWLS
ϵ_V	0.58	0.56	0.54	0.48	0.44	0.45
ϵ_θ	9.07	3.38	2.08	5.28	2.91	2.42
ϵ_P	4.76	1.55	1.07	2.68	1.31	1.14
ϵ_Q	4.79	1.99	1.22	2.97	1.66	1.40
ϵ_{PF}	7.02	2.45	1.52	3.87	1.99	1.76
ϵ_{QF}	7.14	3.18	1.65	4.19	2.44	1.97

TABLE VII
COMPUTATION TIME STATISTICS

Statistic	WLS (a)	WLS (b)	DWLS (a)	DWLS (b)
Average (s.)	0.859	0.910	1.169	1.185
Stand. dev. (s.)	0.198	0.221	0.421	0.438
Minimum (s.)	0.352	0.431	0.507	0.491
Maximum (s.)	1.282	1.493	2.271	2.592

substations at a time, i.e., each processed measurement scenario (of each one of the two sets) is populated with errors originated by the three considered errors corrupting the input measurements.

In order to achieve a better comparison, the results of a WLS estimation using a measurement set free of gross errors is provided. Those results are labeled as WLS*. Results are provided in Fig. 7 and Table VI.

The following observations are in order:

- 1) From Fig. 7, note that the number of misidentifications using the proposed procedure is significantly smaller than using the traditional one. Particularly, if gross errors only affect voltage transformers, only 4% of the suspected measurements are misidentified.
- 2) From Table VI, note that the relative errors of the proposed method are smaller than those of the traditional one and those of the WLS estimator without the bad measurements.

From the computational point of view, as reported in [18], the DWLS algorithm comprises two estimations. Thus, the computational burden of a single DWLS estimation is about twice heavier than that of the traditional WLS method. On the contrary, the number of detection/identification iterations is larger for the traditional WLS bad data detection/identification technique.

Table VII provides computational time statistics for both estimators, using MINOS 5.5 [22] under GAMS [23] on a Linux-based server with four processors clocking at 2.6 GHz and 32 GB of RAM.

Note that the required computation time for the DWLS algorithm is moderately larger than that of the traditional WLS algorithm.

VI. CONCLUSION

If the signal provided by a current or voltage transformer is affected by a gross error, the measurement set used by the state estimator can be corrupted by multiple bad data. In such situation, the performance of the traditional identification algorithm based on the LNR test can be significantly improved if the procedure is modified to consider the statistical correlations between measurements. An insightful analytical example illustrates the proposed methodology, and its comparatively improved performance is demonstrated through two case studies. Future research will focus on multiple bad data identification using the method proposed in [24]. This efficient algorithm is based on evaluating the coherency between the measurement with the largest normalized residual and the rest of the measurements.

REFERENCES

- [1] F. C. Schweppe and J. Wildes, "Power system static state estimation. Part I: Exact model," *IEEE Trans. Power App. Syst.*, vol. PAS-89, no. 1, pp. 120–125, Jan. 1970.
- [2] F. C. Schweppe and D. Rom, "Power system static state estimation. Part II: Approximate model," *IEEE Trans. Power App. Syst.*, vol. PAS-89, no. 1, pp. 125–130, Jan. 1970.
- [3] F. C. Schweppe, "Power system static state estimation. Part III: Implementation," *IEEE Trans. Power App. Syst.*, vol. 89, no. 1, pp. 130–135, Jan. 1970.
- [4] F. C. Schweppe and E. D. Handschin, "Static state estimation in electric power systems," *Proc. IEEE*, vol. 62, no. 7, pp. 972–982, Jul. 1974.
- [5] A. Monticelli, "Electric power system state estimation," *Proc. IEEE*, vol. 88, no. 2, pp. 262–282, Feb. 2000.
- [6] A. Abur and A. G. Expósito, *Electric Power System State Estimation. Theory and Implementations*. New York: Marcel Dekker, 2004.
- [7] W. Liu, F. Wu, and S. Lun, "Estimation of parameter errors from measurement residuals in state estimation," *IEEE Trans. Power Syst.*, vol. 7, no. 1, pp. 81–89, Feb. 1992.
- [8] W. E. Liu and S. Lim, "Parameter error identification and estimation in power system state estimation," *IEEE Trans. Power Syst.*, vol. 10, no. 1, pp. 200–209, Feb. 1995.
- [9] O. Alsac, N. Vempati, B. Stott, and A. Monticelli, "Generalized state estimation," in *Proc. 20th Int. Conf. Power Industry Computer Applications*, 1997, pp. 90–96.
- [10] K. Clements and A. Costa, "Topology error identification using normalized Lagrange multipliers," *IEEE Trans. Power Syst.*, vol. 13, no. 2, pp. 347–353, May 1998.
- [11] A. Expósito and A. de la Villa Jaen, "Reduced substation models for generalized state estimation," *IEEE Trans. Power Syst.*, vol. 16, no. 4, pp. 839–846, Nov. 2001.
- [12] E. Caro, A. J. Conejo, and A. Abur, "Breaker status identification," *IEEE Trans. Power Syst.*, vol. 25, no. 2, pp. 694–702, May 2010.
- [13] A. Abur and M. Çelik, "Least absolute value state estimation with equality and inequality constraints," *IEEE Trans. Power Syst.*, vol. 8, no. 2, pp. 680–686, May 1993.
- [14] L. Mili, V. Phaniraj, and P. Rousseeuw, "Least median of squares estimation in power systems," *IEEE Trans. Power Syst.*, vol. 6, no. 2, pp. 511–523, May 1991.
- [15] S. Mohagheghi, R. Alaileh, G. Cokkinides, and S. Meliopoulos, "A laboratory setup for a substation scaled model," in *Proc. 2007 Power Tech.*, Lausanne, Switzerland, Jul. 2007.
- [16] S. Mohagheghi, R. Alaileh, G. Cokkinides, and S. Meliopoulos, "Distributed state estimation based on the supercalibrato concept—Laboratory implementation," in *Proc. 2007 IREP*, Charleston, SC, Aug. 2007.
- [17] E. Caro, J. M. Morales, A. J. Conejo, and R. Mínguez, "Calculation of measurement correlations using point estimate," *IEEE Trans. Power Del.*, vol. 25, no. 4, pp. 2095–2103, Oct. 2010.
- [18] E. Caro, A. Conejo, and R. Mínguez, "Power system state estimation considering measurement dependencies," *IEEE Trans. Power Syst.*, vol. 24, no. 4, pp. 1875–1885, Nov. 2009.
- [19] Multifunction Meter DM9200, Td ed., Artech, Jul. 2005. [Online]. Available: <http://www.artec.com>.

- [20] R. Mínguez, A. Conejo, and A. S. Hadi, "Non-Gaussian state estimation in power systems," in *Advances in Mathematical and Statistical Modeling*, B. C. Arnold, Ed. *et al.* Boston, MA: Birkhäuser, 2008, pp. 141–156.
- [21] E. Caro, A. J. Conejo, and R. Mínguez, "A sensitivity analysis method to compute the residual covariance matrix," *Elect. Power Syst. Res.*, vol. 81, no. 5, pp. 1071–1078, May 2011.
- [22] A. Drud, "MINOS: A solver for large-scale nonlinear optimization problems," in *The Solvers Manual*. Washington, DC: GAMS Development Corp., 2008.
- [23] A. Brooke, D. Kendrick, A. Meeraus, R. Raman, and R. E. Rosenthal, *GAMS: A Users Guide*. Washington, DC: GAMS Development Corp., 2008. [Online]. Available: <http://www.gams.com/>.
- [24] A. Monticelli and A. Garcia, "Reliable bad data processing for real-time state estimation," *IEEE Trans. Power App. Syst.*, vol. PAS-102, no. 5, pp. 1126–1139, May 1983.



Eduardo Caro (S'08) received the Electrical Engineering degree from the Polytechnical University of Cataluña, Barcelona, Spain, in 2007. He is currently pursuing the Ph.D. degree at the Universidad de Castilla-La Mancha, Ciudad Real, Spain.

His research interests include power system state estimation, optimization, sensitivity analysis, and power system quality.



Antonio J. Conejo (F'04) received the M.S. degree from the Massachusetts Institute of Technology, Cambridge, in 1987 and the Ph.D. degree from the Royal Institute of Technology, Stockholm, Sweden, in 1990.

He is currently a full Professor at the Universidad de Castilla-La Mancha, Ciudad Real, Spain. His research interests include control, operations, planning and economics of electric energy systems, as well as statistics and optimization theory and its applications.



Roberto Mínguez received the Civil Engineering degree and the Ph.D. degree in applied mathematics and computer science from the Universidad de Cantabria, Santander, Spain, in 2000 and 2003, respectively.

During 2004, he worked as a Visiting Scholar at Cornell University, Ithaca, NY, under the Fulbright program. He is currently an Assistant Professor at the Environmental Hydraulics Institute, IH, Universidad de Cantabria, Cantabria, Spain. His research interests are reliability engineering, sensitivity analysis, numerical methods, and optimization.

Marija Zima (S'02–M'08) received the B.Sc. and Ph.D. degrees from the Riga Technical University, Riga, Latvia, in 2002 and 2007, respectively.

In 2000–2005, she was a Planning Engineer at the National power utility Latvenergo. In 2005, she started her Ph.D. studies at ETH Zürich. In 2010, she joined ABB Switzerland, Corporate Research, Zürich.

Göran Andersson (M'86–SM'91–F'97) received the M.S. and Ph.D. degrees from the University of Lund, Lund, Sweden, in 1975 and 1980, respectively.

In 1980, he joined ASEA's, now ABB, HVDC division, and in 1986, he was appointed full Professor in electric power systems at the Royal Institute of Technology (KTH), Stockholm, Sweden. Since 2000, he has been a full Professor in electric power systems at the Swiss Federal Institute of Technology (ETH), Zürich, Switzerland, where he heads the powers systems laboratory.

Dr. Andersson is a member of the Royal Swedish Academy of Engineering Sciences and Royal Swedish Academy of Sciences.